Review

Atmospheric Modelling of Mercury in the Southern Hemisphere and Future Research Needs: A Review

Jorge Leiva González [1,]*, Luis A. Diaz-Robles [1], Francisco Cereceda-Balic [2], Ernesto Pino-Cortés [3] and Valeria Campos [1]

1   Departamento de Ingeniería Química, Universidad de Santiago de Chile, Santiago de Chile 9170022, Chile; alonso.diaz.r@usach.cl (L.A.D.-R.); valeria.campos@usach.cl (V.C.)
2   Centre for Environmental Technologies and Department of Chemistry, Universidad Técnica Federico Santa María, Valparaíso 2390136, Chile; francisco.cereceda@usm.cl
3   Escuela de Ingeniería Química, Pontificia Universidad Católica de Valparaíso, Valparaíso 2362854, Chile; ernesto.pino@pucv.cl
*   Correspondence: jorge.leiva.g@usach.cl

Abstract: Mercury is a toxic pollutant that can negatively impact the population's health and the environment. The research on atmospheric mercury is of critical concern because of the diverse process that this pollutant suffers in the atmosphere as well as its deposition capacity, which can provoke diverse health issues. The Minamata Convention encourages the protection of the adverse effects of mercury, where research is a part of the strategies and atmospheric modelling plays a critical role in achieving the proposed aim. This paper reviews the study of modelling atmospheric mercury based on the southern hemisphere (SH). The article discusses diverse aspects focused on the SH such as the spatial distribution of mercury, its emissions projections, interhemispheric transport, and deposition. There has been a discrepancy between the observed and the simulated values, especially concerning the seasonality of gaseous elemental mercury and total gaseous mercury. Further, there is a lack of research about the emissions projections in the SH and mercury deposition, which generates uncertainty regarding future global scenarios. More studies on atmospheric mercury behaviour are imperative to better understand the SH's mercury cycle.

Keywords: atmospheric mercury; Minamata Convention; southern hemisphere; air pollution; mercury air modelling

1. Introduction

The increments in the concentration of atmospheric pollutants have generated problems for people's health and the environment [1]. One toxic pollutant that can harm the humans is mercury. In addition, low concentrations of this metal can severely damage people's health and lead to conditions such as cardiovascular or reproductive illnesses. However, the adverse effects of this metal depend on diverse factors such as exposure or chemical composition; therefore, to investigate the mercury cycle, current and future levels are relevant [2]. Although mercury in the atmosphere comes from natural processes such as volcanic activity, anthropogenic activities, such as stationary coal combustion or the gold mining industry, are the main sources of mercury release into the environment and disrupt the natural cycle of mercury [2]. Although mercury can be present in the air, water, and on the ground, a large amount of anthropogenic mercury pollution reaches the atmosphere and enters ecosystems through dry and wet deposition. The study of mercury has become relevant in the last 30 years and there have been diverse scientific events related to mercury since 1990 [3]. However, one of the main initiatives that encourages the protection of the environment and the population's health is the Minamata Convention on Mercury. This convention started in 2017 and was implemented based on scientific reports from the International Conference on Mercury as a Global Pollutant (ICMGP) [3]. Between the

35 articles of the convention, the scientific contribution is crucial for the success of their goals. To illustrate, the articles of the Minamata Convention include mercury emissions in air (article 7), reinforcing mercury monitoring systems (article 15), providing mercury data baselines (article 19), and enhancing modelling techniques (article 20), among others [3,4].

One of the main adverse issues of mercury is the bioaccumulation that it can have. Although atmospheric mercury can deposit on land and water, the surfaces remit part of it into the atmosphere [4]. However, another percentage is methylated and deposited into the ecosystem. Indeed, inorganic mercury can be methylated and bioaccumulated in aquatic environments and biomagnified in the aquatic food chain [5,6]. In this context, although found in several types of foods, researchers measured the levels of mercury; fish revealed higher levels of this mental. Fish are one of the most crucial exposure routes for humans [2,5]. Fish bioaccumulate methylmercury in their muscle tissues; however, higher levels of mercury were found in some fish species such as swordfish, tilefish, and sharks. Therefore, people with a diet based on fish and marine mammals could have greater exposure to mercury [2].

Mercury in the atmosphere can be in diverse phases, such as gas and solid particles (clouds and aerosols). In the atmosphere, this element can be found as gaseous oxidized mercury (GOM), Hg^2, particulate-bound mercury (PBM), and gaseous elemental mercury (GEM), Hg^0 [6–9]. GEM is the more abundant form in the atmosphere, which is relatively inert. Indeed, it can travel long distances before it is modified with oxidation chemical reactions in the atmosphere or removed by some receptors such as those in plants [5]. In contrast, the fastest deposition occurs for oxidized mercury compounds because of their greater solubility in water. For this reason, GOM and GEM can negatively affect local ecosystems unlike elemental mercury, which is less reactive and has a long lifetime [10]. Although the pollutant can be found in three forms, there are several transformation phenomena in which mercury suffers as well as in transport. Besides oxidation and reduction reactions, complex formations occur and phases change, especially when there is an interaction between the atmosphere and the ocean, bioaccumulation, and between other phenomena [11].

Atmospheric modelling plays a crucial role in reaching the Minamata Convention aims. In this respect, meteorological and air quality modelling help to predict and forecast using current data, meteorological phenomena, and the behaviour of the concentration of various pollutants [12,13]. In particular, there is a lack of real-time studies of certain compounds, such as mercury, and models for predicting air quality and for simulating and studying diverse scenarios [12]. The equations that govern atmospheric modelling consider several parameters such as pressure, temperature, speed, and concentration, among others. Hence, developing a model requires supercomputers to perform the simulations for a precise and detailed prediction because of the spatial variations in the parameters [12,13]. Various meteorological and air quality models have been used to study different pollutants including mercury. However, for atmospheric mercury, most of the investigations are on a global scale or in the Northern Hemisphere (NH) [5,8,14–17]. The main reason for this is the information available. There are several places measuring mercury in the NH in contrast to the Southern Hemisphere (SH) where there is a deficient number [8,14,18]. In fact, in the SH, there are six monitoring sites, of which only one in Australia measures the wet deposition of mercury. In contrast, in the NH, 123 sites measure wet deposition [14]. This situation increases the complexity of comparing the results of simulations with observed data.

Chemical transport models (CTM) can study how the atmosphere is affected by the pollutants emitted, mathematically exposing diverse phenomena such as transport caused by wind and dispersion caused by turbulent movements, among others [19]. For mercury, CTM are highly relevant because of the lack of real-time measurements of this compound and the problems it can cause for people's health [5]. In recent decades, atmospheric models have been developed analysing mercury, considering O_3, OH radicals, and halogen species as the primary oxidants of Hg^0. However, there is still a discrepancy about which oxidant is dominant [20]. The main pathway oxidations used for Hg^0 are OH/O_3 and Br

where adequate results have been obtained. However, mercury chemistry, for which there are multiple Hg^0 oxidants, is more complex [20]. Using CTMs in mercury atmospheric predictions has some advantages. For instance, it is possible to evaluate potential policy outcomes to estimate and analyse the changes in relevant factors such as mercury deposition. These models also allow the evaluation of proposed measures to determine their potential efficacy in mercury abatement or worldwide reduction [21]. Further, CTMs can give wide regional and seasonal variations in Hg^0 concentrations to compensate for the absence of real-time observed data. Accurate global estimates of mercury dispersion can be obtained by reproducing the time and spatial patterns of mercury measurements [21,22]. However, CTMs also have some disadvantages. Indeed, when different atmospheric redox mechanisms are included in the models, recent investigations have shown that it is still difficult to reproduce the patterns of the observed concentrations [21]. One area where uncertainty persists is the potential importance of heterogeneous chemistry, an aspect that models have been unsuccessful at incorporating. The uncertainty of emissions inventories is another problem with CTMs. The dependence on inventory data, particularly the amount of mercury released from natural sources, has become a significant obstacle in studies of atmospheric models [21–23].

1.1. Emissions of Mercury

Estimates of anthropogenic mercury emissions have a particular uncertainty. The principal reasons are the lack of precision in the estimation methods, the low participation of some countries in the estimation of emissions, and the lack of consideration of specific activities in the estimation of mercury's emissions inventory [9]. However, some studies suggest a consensus regarding the main sources of anthropogenic mercury emissions. In 2015, the highest emissions were from small-scale gold mining, followed by the combustion of fuels for different uses, and industry sectors. Further, compared to the global mercury emissions of anthropogenic sources from 2010 to 2015, they increased by 410 Mg/year [21,24]. China is the country with the highest level of mercury emissions [24]. Figure 1 presents the trends in global mercury emissions with anthropogenic origins from 1990 to 2015. During 2010 and 2015, there were no significant changes in the emissions patterns. The most significant emissions come from Asia for both years, representing around 48.8%, followed by South America with 18.4% and 16.2% from sub-Saharan Africa. The region with the most significant anthropogenic mercury emissions is East and Southeast Asia with 859 Mg/year, representing 38.6% of the total. In addition, regarding fixed emissions sources, fossil fuel combustion and biomass burning represent around 24% of global mercury emissions [21].

The global emissions inventory of mercury into the atmosphere from anthropogenic sources is estimated to be close to 2220 Mg/year [21]. Gold mining, including artisanal and small-scale, is responsible for around 838 Mg/year, followed by diverse industrial sectors with 613.6 Mg/year, and the combustion of fuels to produce energy for different uses is responsible for 481 Mg/year [21]. Table 1 shows the details of the three sectors and the various subdivisions and sources of each sector. This table illustrates that 99.53% (2189.7 Mg/year) of the total mercury emissions come from anthropogenic sources (1932.6 Mg/year). In the SH, around 68% of the anthropogenic mercury emissions come from artisanal and small-scale gold mining (ASGM). Also, most of the emissions come from the latitudes +30° to −30° [25]. Most of the emissions for ASGM are from South America, with 340 Mg/year, representing 40.6% of the total for this sector group, where Peru has the highest emissions with 110.4 Mg/year [21]. In addition, African countries are responsible for about 30.1% of the ASGM mercury emissions (252 Mg/year); however, the countries in the SH of the continent represent around 22% of the African contribution. Regarding Oceania, this continent does not register emissions for the ASGM sector. Further, some countries partly in the SH have high mercury emissions levels in the ASGM sector, such as Indonesia, with 124.5 Mg/year [21,26].
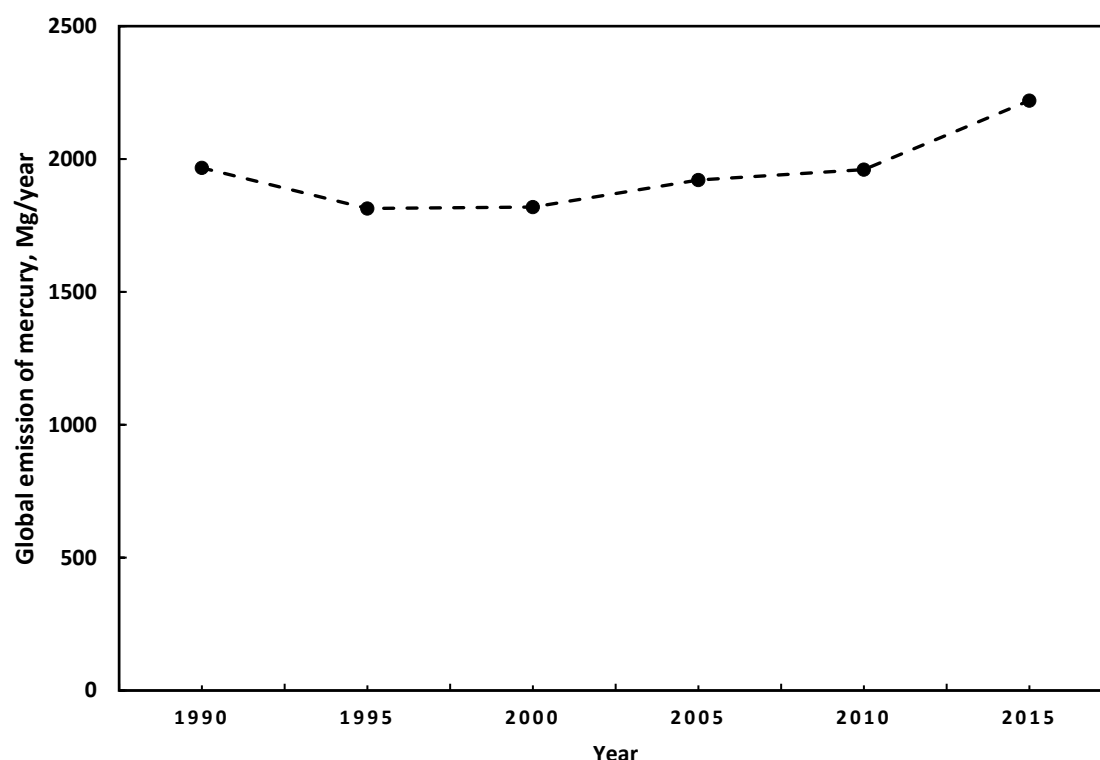
Figure 1. The trend in the global emissions of mercury to air from anthropogenic sources [21,27].

The percentage contribution between anthropogenic and natural emissions depends on the model used to estimate the emissions. Indeed, the anthropogenic/natural ratio can be different for diverse models. For instance, using the GEOS-chem model, the ratio could be 0.583 and using the GRAHM model it could be 0.629 [9]. However, considering a natural emissions estimation for 2008, the emissions are about 5207 Mg/year [9,28,29]. Using the most recent estimation for anthropogenic emissions, which was 2200 Mg/year [21], the total mercury emissions could be around 7407 Mg/year, of which the natural contribution is around 70.30% providing an anthropogenic/natural emissions ratio of 0.423. However, there is uncertainty associated with the estimation of both anthropogenic and biogenic emissions. This is because of differences in emissions factors, uncertainties in emissions reports from some countries, and comparisons of emissions with field measurements [29]. With biogenic sources, it is necessary to consider two aspects. The mercury emissions emitted directly from natural processes are the primary sources such as volcanic emissions. Further, the secondary sources are the re-emissions of this metal because of a previously accumulated deposition on both marine and terrestrial surfaces such as biomass burning [28]. For the natural sources of mercury, Table 1 shows the details of the estimations for global emissions by 2008. In that case, the most significant contribution was made by remissions from the oceans with 2682 Mg/year, followed by biomass burning with 675 Mg/year, and deserts and metalliferous and non-vegetated zones with 546 Mg/year. Indeed, most of the natural emissions come from the remission process, representing a considerable proportion of the total mercury emissions. For instance, oceans and biomass burning from natural sources represent around 45.32% of the total mercury emissions inventory [28,29].

Table 1. Main sectors of anthropogenic mercury emissions (A) and natural emissions (N). The anthropogenic emissions to the atmosphere are for 2015 and based on 2200 Mg/year and the table shows 99.53% of the total anthropogenic emissions [21]. The natural emissions are for 2008 and based on 5207 Mg/year; adapted from Pirrone et al. (2010) [9,28,29].

Source	Type	Sector	Emissions Mg/Year	Contribution %
Artisanal gold production	A	Artisanal and small-scale gold mining	838	11.31%
Combustion of fuels (energy, industry, and domestic/residential uses)	A	Stationary combustion of coal for transportation, domestic, and residential.	55.8	0.75%
		Stationary combustion of gas for transportation, domestic, and residential.	0.165	0.00%
		Stationary combustion of oil for transportation, domestic, and residential.	2.7	0.04%
		Industrial stationary combustion of coal.	126	1.70%
		Industrial stationary combustion of gas.	0.123	0.002%
		Industrial stationary combustion of oil.	1.4	0.02%
		Power plants' stationary combustion of coal	292	3.94%
		Power plants' stationary combustion of gas	0.349	0.002%
		Power plants' stationary combustion of oil	2.45	0.03%
Diverse industrial sectors	A	Raw materials and fuel for cement production (excluding coal)	233	3.15%
		Production of non-ferrous metals, including Al, Cu, Pb and Zn	228	3.08%
		Gold production on a large scale	84.5	1.14%
		Production of mercury	13.8	0.19%
		Refining of oil	14.4	0.19%
		Production of steel and pig iron (primary)	29.8	0.40%
		Secondary production of steel	10.1	0.14%
Biomass burning	A	Biomass burning from domestic, industrial, and power plants	51.9	0.70%
Waste	A	Other waste	147	1.98%
Vinyl-chloride monomer	A	Vinyl-chloride monomer production (mercury catalyst) and vinyl-chloride monomer recycling	58.2	0.79%
Oceans	N	Re-emissions from the ocean	2682	36.21%
Biomass Burning	N	Emissions from accumulated mercury in biomass	675	9.11%
Arid areas	N	Deserts and metalliferous and non-vegetated zones	546	7.37%
Tundra/Grassland/Savannah	N	Tundra/Grassland/Savannah	448	6.05%
Forests	N	Forests	342	4.62%
Evasion after mercury depletion events	N	Evasion after mercury depletion events	200	2.70%
Agricultural areas	N	Areas with agricultural processes	128	1.73%
Lakes	N	Lakes	96	1.30%
Geothermal activities	N	Volcanoes and geothermal activities	90	1.22%

Regarding biomass burning mercury emissions (BBME) from natural sources, Africa is the most significant contributor, followed by Asia, and then the Americas with 41%, 31%, and 28%, respectively [30]. Indeed, there is also an essential contribution from the SH. Considering the annual emissions of 675 Mg of mercury, equatorial Asia has around 28.44%, followed by boreal Asia with 14.67%, and the southern part of South America with 14.07%.

To summarise, about 53% of the BBME comes from the SH [31]. The vegetation plays a crucial role in the BBME because of forest fires. Shi et al. (2019) related the most significant amount of mercury emissions to forest fires from tropical forests [30]. Tropical forests are found to a greater extent in SH areas such as Bolivia, Central Africa, and the central region of Brazil, in addition to NH areas such as Laos, Cambodia, and Myanmar [30]. The second type of vegetation with a high level of BBME is woody savanna/shrubland. It is mainly found in Africa, concentrated in Central Africa and East Africa, in addition to Cambodia and Myanmar [30].

1.2. Mercury and Health Effects

Although the atmosphere is the most relevant transport route for mercury, the processes and phenomena that occur on land and in the oceans play a relevant role in its redistribution. Methylmercury (CH_3Hg) becomes relevant as the principal route of human exposure is through the consumption of fish [32]. This neurotoxic contaminant can provoke specific adverse health effects such as cardiovascular or neurocognitive illnesses. For instance, through food consumption, which is the primary exposure route, a study in China attributed around 10,000 deaths per year because of heart attacks provoked by this metal [33]. The negative impact of mercury on humans depends on diverse factors such as chemical composition, exposure time, and concentration. Among the health issues are impaired neurological development, arrhythmias, cardiomyopathy, and kidney damage. In addition, high doses of mercury vapour inhalation can cause respiratory failure [2].

There are four broad categories into which it is possible to divide the health effects that mercury exposure can produce. These are neurological, renal, cardiovascular, and reproductive problems. Regarding the neurological effects, some studies have shown that prolonged exposure to mercury in low doses can cause sleep disorders, mood changes, and various neurological diseases [2,34]. For example, adverse effects have been found with levels of inorganic mercury in urine close to <4 µg/L [2]. Another neurological problem is memory loss because of the deactivation of enzymes required to produce energy in brain cells. In addition, studies have shown that mercury is neurotoxic, which is why it can cause significant damage to the brain and nerve cells [2,35].

Regarding the negative effects at the kidney level, mercury affects not only human beings but also other mammals because the kidneys accumulate mercury ions. Unlike organic mercury compounds, oral exposure to inorganic mercury salts at low and prolonged doses can generate a significant accumulation of this metal resulting in kidney failure [36]. Regarding the cardiovascular effects, exposure to toxic levels of mercury can cause various illnesses such as an increased heartbeat, irregular pulsations, and even high blood pressure [2]. Some studies have shown a correlation between the intake of mercury through the frequent consumption of fish and the increase in the blood pressure of specific patients. In addition, a specific correlation between mercury exposure and an increased risk of hypertension and myocardial infarction has been detected [37]. The last aspect is the reproductive problems that mercury exposure can cause. Some authors have shown that this metal can negatively affect the reproductive functions of men and women. Other studies suggest that long mercury exposure can lead to a generation of congenital disabilities because of its toxicity [2].

Some investigations have demonstrated mercury's negative effects based on previous health issues. In the SH, some relevant health issues are related to the main anthropogenic atmospheric mercury sources. In Palu city in Indonesia, a country partially in the SH, research has detected a high GEM level in that city close to ASGM activities, reaching between 2.06 and 375 ng/m^3. It was determined that the high exposure to GEM was an elevated human health risk for residents [38]. In Bolivia, because of ASGM processes, there are high risks to the population's health in the mountain zones close to the mining operations. The two mining sites studied had levels of mercury vapour that exceeded the EPA's recommended concentration [39]. In addition, settlements close to the mining operations have detected levels of Hg and some families burn Hg amalgam in their homes

without respiratory protection. In that research, the authors concluded that there was a high risk of cancerous and non-cancerous health problems for the population in the studied area [39].

A study in Tanzania showed the high risk faced by gold mine workers and local communities because of Hg exposure [40]. Research participants who were highly exposed to Hg reported medical symptoms, such as tremors in diverse body parts, sensory disturbances, and coordination problems. Long-term mercury exposure causes symptoms related to central and peripheral nervous system damage [40]. Another case is Chile, where a study of children in rural schools showed that long-term mercury exposure can impact children's motor skills [41]. The rural areas studied were near ASGM activities, where the population has been constantly exposed to atmospheric mercury even though mining companies have implemented diverse environmental management strategies to reduce pollution [42]. The authors argued that children exposed to Hg burning could have pathological pure motor skills because of an alteration in the central nervous system [41]. Another case is Ecuador, where a study on children in a mining area detected high mercury concentrations. The mean mercury concentration in the blood was close to 3.23 μg/L [43]. The authors identified these elevated mercury levels in children in urban and rural areas near gold mining activities [44]. In another place in Ecuador, Portovelo, an investigation detected a high mercury concentration level in the air. Researchers identified that in urban areas near the mining operations, atmospheric mercury levels were beyond the defined dangerous concentration level (around 200 ng/m^3) [45]. In the places described in this section, the health of the populations are at risk. The levels of mercury detected in areas close to ASGM activities, in most cases, exceeded current regulations. In this sense, educating the population about the negative effects of mercury exposure is essential. Further, there is a need to prevent the adverse effects on communities, especially the neurotoxicity effect it can have on children [44,45].

2. Modelling Atmospheric Mercury

Several meteorological and air quality models have been used to study atmospheric mercury. However, most of the investigations have been developed at a global level or the NH level. This problem begins with the information since, although several places measure atmospheric mercury globally, the number of monitoring stations is lower (6). Indeed, only one station in Australia measures wet mercury deposition. In contrast, in the NH, 123 sites measure wet mercury deposition. This situation increases the complexity of comparing the results of simulations with the observed data. Despite this, researchers have developed several studies based on global simulations to study the behaviour of mercury in both the NH and SH [14]. In this sense, they seek to improve the information available in both hemispheres, promoted mainly by the Minamata Convention. Since the convention, various researchers have worked to increase the knowledge about this contaminant to better understand the mercury cycle and how it is affected by anthropogenic emissions. The Minamata Convention seeks to promote research to support decision making and adequate management to reduce pollution associated with mercury. Mathematical models are relevant among the subjects of the convention to evaluate the effects that could provoke mercury emissions variations. Therefore, mercury atmospheric modelling is of enormous relevance to the aims of the Minamata Convention [3,4].

2.1. General Aspects

At a global level, one of the most frequently used CTM has been GEOS-CHEM to explore the behaviour of mercury in both the NH and SH [14,15,46–59]. However, other CTM have been used to explore atmospheric mercury such as WRF-CHEM [60,61] and ECHMERIT [14,26,62–64]. Through those CTM, researchers have examined diverse aspects such as wet and dry deposition or mercury concentration in its different states in the atmosphere. Most of the CTM investigations are at the global level or at specific sites in the NH. However, some of the studied places have been in the SH, such as Australia, or sites

with mercury measurement stations such as Cape Point (CPT) or Amsterdam Island (AMS). Therefore, this section explores and analyses those investigations as they provided some relevant aspects of the atmospheric modelling of mercury in the SH.

One aspect reviewed in the research was the oxidation mechanisms of GEM. Regarding GEM oxidation, most chemical transport models assume that the predominant oxidants are OH and O_3. The OH radical plays a fundamental role in the oxidation of organic and inorganic components in the atmosphere. However, OH only represents 1% of the global oxidation of Hg^0 in contrast to Br, which is associated with 97% of the oxidation of elemental mercury [47,48]. In addition, an aspect to consider is the lower concentration of O_3 in the SH compared to the NH. Therefore, this compound has more significant participation in the oxidation of GEM in the NH than it does SH. Indeed, the chemical mechanisms used can highly influence the CTM. For example, for reactive mercury (RM), models that used OH and O_3 as the main oxidants predict higher RM concentrations than others for low latitudes.

On the contrary, models that used Br in their chemical mechanisms generated patterns of higher concentrations for RM in the SH [14,47,48]. Regarding the results in the SH for the investigation, which used OH and O_3 as the main oxidants of Hg^0 in the gas phase [62,65], Pacyna et al. (2016) identified two zones in the SH with high values of GEM. The first is the central part of South America, with values between 1.6 and 2.4 ng/m^3. This region is between latitudes $-20°$ and $0°$, specifically Bolivia and part of the Amazon. The other area is in southern Africa (between latitudes $-40°$ and $0°$), which has similar values to the previous region. However, they identified a maximum peak in South Africa with values between 2.4 and 2.8 ng/m^3 [62].

In contrast, a model presented by Travnikov et al. (2017), which used Br as the main oxidant, showed slightly different GEM values. In latitudes $-40°$ and $0°$, the southern part of Africa presented values between 1.3 and 1.6 ng/m^3. The values for the central part of South America (latitudes $-20°$ and $0°$) were between 1.3 and 2.4 ng/m^3. Similarly, this study recognized a maximum peak in South Africa; however, this was lower since the GEM values were close to 2.4 ng/m^3 [14,62,65]. When compared to the previous research, although the GEM levels had the same order of magnitude for the same SH regions, it was possible to identify some differences. The main reason was the effect generated by the diverse oxidation mechanisms in the CTM. Therefore, there was an evident influence on the results of the atmospheric reduction pathways used. Shah et al., 2021 presented modelling that considered the oxidation mechanisms of Br and OH. This study included intermediate processes (second stage) of oxidation of Hg (I) by O_3 and radicals to form Hg (II) [54]. The maximum peak found in South Africa was among their results, which was consistent with previous studies. In addition, they observed high concentrations of GEM in the northern part of South America, results not presented in the previous modelling, which demonstrated the influence of the chemical mechanisms used [54].

2.2. Spatial Distribution of Mercury

Researchers have studied the spatial distribution of atmospheric mercury several times. They agree with the seasonality in the mercury distribution in its various forms, especially in the NH. However, there are still differences regarding the values obtained on the spatial distribution of atmospheric mercury in the SH [59]. Currently, there is no clarity regarding the seasonal variation in the SH. Some authors have shown that there is a low seasonal variation, whereas others argue that it does not exist. For instance, for total gaseous mercury (TGM), which includes Hg^0 and the gaseous part of Hg (II), Horowitz et al., 2017, analysed a model comparing the values observed in CPT and AMS, finding a non-significant seasonal variation [59]. In Bolivia, a measurement campaign during 2014–2015 found lower TGM values of between 10% and 15% compared to AMS (at similar latitudes). In addition, they detected a seasonality in the studied area, obtaining the lowest TGM values during the driest season (austral winter) and higher values during the wetter seasons (austral summer). This seasonality identified in Bolivia, the central

part of South America, disagrees with the results obtained from other subtropical and mid-latitude sites in the southern hemisphere, such as AMS and CPT [66]. Another study was the global simulation by Huanxin Zhang et al. (2021). In this study, the observed TGM values were compared with the simulated ones, producing errors of approximately 13% for the TGM values in the SH. However, only the seasonal variation pattern of the NH agreed with previous studies. The highest values for the TGM were during the winter of the NH (December to March) and the lowest values were during summer in this hemisphere (June to September) [55]. In the investigation, they studied the Neumayer station (Antarctic) in the SH. When comparing the data observed for the year 2000 with the model carried out, they observed an opposite seasonality between them. The highest peak in the observed data was during the austral summer and the model was made during the austral winter [55].

Another study [67] detected no seasonality of the GEM in the SH. In this investigation, they found higher seasonal amplitudes in terrestrial sites, which were related to the vegetation relevance to the absorption of Hg^0. Indeed, vegetation serves as a sink during the summer and is a source of emissions in winter. Despite the above, in the observed data, they detected a low seasonal variability in the station in Bariloche (BAR), Patagonia, Argentina, where there was a low oscillation of Hg^0 during summer and autumn [67]. For the GEM, some measurements in the SH sometimes showed a specific seasonal variability such as in the Antarctic, with higher values during winter and spring [68]. This is complex to reproduce in the CTM because of the lack of data on the seasonal variations in anthropogenic emissions in the SH [14]. However, some authors have found a clear seasonality in SH. For example, Song et al. (2015) for the GEM in the simulation showed that the concentrations varied according to the season analysed. They found high values for the southern winter of around 1.3 ng/m^3 and low concentrations for the southern summer, close to 0.9 ng/m^3 [69]. Thus, the global models have shown a low capacity in the SH to accurately represent the concentrations observed in the different measurement sites and the seasonality [70]. Despite this, Zhou et al. (2021) in their research through modelling presented for 2015 (GEM-MACH-Hg), considered the vegetation uptake a significant mercury removal pathway. They developed two models with and without vegetation cover, obtaining similar results to the observed data in the four stations in the SH. Although the observed data largely agree with the models in this modelling, there are specific differences. For example, the model could not show the seasonality present at Gunn Point, Australia. During the summer, there are differences of close to 30% between the modelled values and the observed values. In this case, it does not illustrate the wide variations that exist in the period between June and September [18].

Table 2 shows the details of the TGM and GEM data obtained with the simulation models for different places in the SH. Table 3 shows the details of the TGM and GEM data obtained using the measurement methods. In both tables, is it possible to see some discrepancies between the modelling and measurement values.

Table 2. Different values for TGM and GEM were obtained by simulation models for the SH. To achieve values for each season, the data for * studies are interpreted from graphs and tables. The seasons are summer between January and March, Autumn between April and June, Winter between July and September, and Spring between October and December.

Location	Lat (°)	Long (°)	Period	TGM, ng/m^3	GEM ng/m3	Studied Years	Used Model	Reference
Amsterdam Island	−37.80	77.55	Summer Autumn Winter Spring		0.93 1.15 1.31 0.99	2009–2011	GEOS–Chem	[69] *
			Summer Autumn Winter Spring	0.97 1.07 1.05 0.93	0.95–1.0 1.0–1.1 1.1–1.05	2015	GEM–MACH–Hg model Uptake of Hg by vegetation is considered.	[18] *

Table 2. *Cont.*

Location	Lat (°)	Long (°)	Period	TGM, ng/m^3	GEM ng/m3	Studied Years	Used Model	Reference
Cape Point	−34.35	18.49	Summer Autumn Winter Spring		0.95 1.15 1.3 0.98	2009–2011	GEOS–Chem	[69] *
			Summer Autumn Winter Spring	1.08 1.03 1.03 1.03		2007–2008	GEOS–Chem (Hg + Br)	[55] *
			Summer Autumn Winter Spring	1.33 1.23 1.17 1.27		2007–2008	GEOS–Chem (Hg + OH/O$_3$)	[55] *
			Summer Autumn Winter Spring	1 1.08 1.05 0.96	0.95–1.05 1.05–1.1 1.1–1.05	2015	GEM–MACH–Hg model Uptake of Hg by vegetation is considered.	[18] *
Amsterdam Island and Cape Point			Summer Autumn Winter Spring	0.67 0.82 1 0.88		2009–2011	GEOS–Chem–MITgcm	[59] *
			Summer Autumn Winter Spring	0.98 1.08 1.04 0.94		2015	GEM–MACH–Hg model Uptake of Hg by vegetation is considered.	[18] *
Troll Research Station, Antarctica	−72	3	Summer Autumn Winter Spring		0.82 1.07 1.23 0.86	2009–2011	GEOS-Chem	[69] *
			Summer Autumn Winter Spring	0.84 0.96 0.96 0.83	0.8–0.9 0.9–1.0 1.0–0.95 0.95–0.8	2015	GEM–MACH–Hg model Uptake of Hg by vegetation is considered.	[18] *
Amsterdam Island, Cape Point and Troll Research Station			Summer Autumn Winter Spring		0.93 1.13 1.28 0.99	2009–2011	GEOS–Chem	[69] *
Neumayer, Antarctica	−70.68	−8.27	Summer Autumn Winter Spring	1.15 0.99 0.97 0.99		2007–2008	GEOS–Chem (Hg + Br)	[55] *
			Summer Autumn Winter Spring	1.36 1.18 1.13 1.26		2007–2008	GEOS–Chem (Hg + OH/O$_3$)	[55] *
ATARS, Gunn Point, Australia	12.25	131	Wet season (December–March) Dry Season (Jun–September)		0.90 ± 0.10 0.97 ± 0.13	2013–2014	GEOS–Chem y HYSPLIT	[46]
			Summer Autumn Winter Spring	1 0.91 0.99 0.99	0.90–0.95 0.95–0.95 0.95–1.0	2015	GEM–MACH–Hg model Uptake of Hg by vegetation is considered.	[18] *
Antarctica	-	-	Annual Average		1.03	2015	Hybrid Single-Particle Lagrangian Trajectory model (HYSPLIT)	[71]
Southern Ocean	-	-	Spatial concentration pattern Spatial concentration pattern		1.0 ± 0.22 0.9 ± 0.38	2014–2015	GEOS–Chem–MITgcm GEOS–Chem–MITgcm–model with improved CMF (cloud mass flux)	[49]
South America	-	-	Annual average		1024	2015	Hybrid Single-Particle Lagrangian Trajectory model (HYSPLIT)	[71]

Table 2. *Cont.*

Location	Lat (°)	Long (°)	Period	TGM, ng/m^3	GEM ng/m3	Studied Years	Used Model	Reference
			Spatial concentration pattern	1.27 ± 0.21		2007–2008	GEOS–Chem	[55]
			Spatial concentration pattern	1.1–1.3		2008–2009	ECHMERIT	[65]
The Southern Hemisphere	-	-	Annual average		0.986	2015	Hybrid Single-Particle Lagrangian Trajectory model (HYSPLIT)	[71]
			Spatial concentration pattern	1.16 ± 0.03		2000	GEOS–Chem	[55]
			Spatial concentration pattern		0.9–1.1	2013	GLEMOS GEOS–Chem GEM–MACH–Hg ECHMERIT	[14]

Table 3. Different observed values for TGM and GEM in the SH. To achieve values for each season, the data for * studies are interpreted from graphs and tables. The seasons are summer between January and March, Autumn between April and June, Winter between July and September, and Spring between October and December. The instrument used to measure atmospheric mercury in the monitoring stations was the Tekran continuous mercury vapour analyser, model 2537A/B.

Location	Lat (°)	Long (°)	Period	TGM, ng/m^3	GEM ng/m^3	Years Studied	Reference
			Summer	-	1.00		
			Autumn	-	0.98	2013	[68]
			Winter	-	1.10		
			Spring	-	1.03		
			Summer		1.02		
			Autumn		1.05	2012–2017	[7] *
			Winter		1.07		
			Spring		1.01		
Amsterdam Island	−37.8	77.55	Annual Average		1.025 ± 0.065	2012	[72]
					1.028 ± 0.096	2013	
			Summer		1.02		
			Autumn		1	2012-2013	[72] *
			Winter		1.07		
			Spring		0.99		
			Annual mean		1.03 ± 0.1	2013–2014	[73]
			Summer	-	0.71		
			Autumn	-	1.01	2013	[68]
			Winter	-	1.00		
			Spring	-	1.03		
			Summer		1.04		
			Autumn		1.02	2012–2017	[7] *
Cape Point	−34.35	18.49	Winter		1.05		
			Spring		1.06		
			Annual Average		1.017 ± 0.095	2012	[72]
					1.052 ± 0.160	2013	
			Summer		0.99		
			Autumn		1.01	2011–2013	[72] *
			Winter		0.99		
			Spring		0.97		
			Annual mean		0.95 ± 0.12	2014–2016	
ATARS, Gunn Point, Australia	12.25	131	Summer		0.82		[46]
			Autumn		0.89	2015	
			Winter		0.98		
			Spring		0.99		

Table 3. *Cont.*

Location	Lat (°)	Long (°)	Period	TGM, ng/m^3	GEM ng/m^3	Years Studied	Reference
Antarctica–Dumont d'Urville	−66.66	140	Annual Average		0.87 ± 0.23	2012–2015	[74]
			Summer	-	0.83		
			Autumn	-	0.89	2013	[68]
			Winter	-	0.74		
			Spring	-	0.33		
Antarctica–Concordia Station	−75.1	123.34	Annual Average		0.76 ± 0.24 / 0.81 ± 0.28	2012 / 2013	[74]
			Summer	-	0.84		
			Autumn	-	1.03	2013	[68]
			Winter	-	0.83		
			Spring	-	0.75		
Troll Research Station, Antarctica	−72	3	Annual Average		1.052 ± 0.160 / 0.970 ± 0.162	2012 / 2013	[74]
			Summer		1.07		
			Autumn		1.03	2011–2013	[72] *
			Winter		1.03		
			Spring		0.92		
Cape Grim	−40.68	144.69	Annual Average		0.872 ± 0.130 / 0.848 ± 0.112	2012 / 2013	[72]
			Summer		0.89		
			Autumn		0.86	2011–2013	[72] *
			Winter		0.89		
			Spring		0.85		
			Annual Average		0.9 ± 0.35	2015–2017	[75]
			Overall Mean–November 3 to November 6		1.03 (±0.16)	2006	
Bariloche	−41.13	−71.42	Summer	-	0.88		
			Autumn	-	0.89	2013	[68]
			Winter	-	0.93		
			Spring	-	0.86		
			Annual mean		0.9 ± 0.14	2014–2015	[73]
			Annual Average		0.86 ±0.16	2012–2017	[6]
Latrobe Valley, Australia	38.18	146.25	Overnight–6 PM–6 AM (May to July)		1.6–1.8 / 1.2–1.3	2013	[60]
The Macquarie University Weather Station, Australia	−33.765	151.117	Annual Average		0.65 ± 0.24	2016–2017	[75]
Chacaltaya Station, Bolivia	16.35	68.13	Overall Mean–normal condition	0.89 ± 0.01		July 2014–May 2015	[66]
			Overall Mean–unusual condition because of the Niño phenomena	1.34 ± 0.01		Jun 2015–February 2016	
Amsterdam Island, Cape Point, Bariloche, Dumont d'Urville, and Concordia Stations			Annual mean	-	0.93	2013	[68]
			Summer	-	0.91		
			Autumn	-	0.96	2013	
			Winter	-	0.92		
			Spring	-	0.92		
Amsterdam Island, Cape Point, Bariloche, and Dumont d'Urville Stations			Annual mean	-	0.97	2014	[68]
			Summer	-	0.92		
			Autumn	-	0.96	2014	
			Winter	-	1.03		
			Spring	-	1.01		

2.3. Projections of Mercury Emissions

Most of the anthropogenic mercury emissions come from the NH. Although there are fewer anthropogenic mercury emissions, the southern part of Africa and central South America significantly contribute to the SH's emissions. Moreover, there is an important contribution from Indonesia, which is principally in the SH. In addition, 29.7% of the mercury emissions are anthropogenic and the remainder is from natural sources [62]. This is because of the amount of recycled mercury already deposited in the soil, vegetation, and oceans called legacy emissions. Thus, if there are no significant changes in atmospheric emissions, mercury deposition could increase because of these legacy emissions. Based on this, it is vital to consider these inherited emissions when carrying out an adequate projection of emissions [15]. However, most models have worked with the assumption that these emissions are constant and the changes depend only on anthropogenic emissions. According to Angot et al. (2018), there may be variations of around 14% in the analysis of global emissions reductions [15].

Research based on the Panel on Climate Change scenarios (IPCC) studied the climate change effect on mercury emissions. Although the focus was on the NH, they developed some analysis of the SH [76]. They used a CAM-Chem CTM, projecting emissions by 2050 for three scenarios, A1FI (upper bounds), A1B (middle bounds), and B1 (lower bounds) [21,76]. They suggested that the mercury anthropogenic emissions would rise. Based on data from the year 2020, the authors estimated an increase of 9% to 173% by the year 2050, with the use of fossil fuels being the main cause of this [76]. Projections showed an increase in TGM concentrations globally by the year 2050. In the SH, the authors identified considerable alterations for the A1B and A1FI scenarios in southern Africa and Central America. Based on the results, the research concluded that the interhemispheric differences could be much greater. Indeed, for both the NH and SH, it could magnify the mean concentrations at mid-latitudes. For the SH, the authors attributed these results to the emissions by the mining industry in Southern Africa. The increase in the mean zonal concentrations of TGM for the SH would be between 0.5 and 1.2 ng/m^3. For the case of latitudes above 60°, the authors suggested that the concentration changes in the TGM are less than half the average in the SH [76].

Pacyna et al. (2016) in their research using two CTM (ECHMERIT and GLEMOS), proposed three scenarios for the projection of mercury emissions by 2035. The first refers to the Current Policy (CP), which considers a slight increase in annual mercury emissions (around +3.02 Mg/year). The second scenario, a New Policy (NP), considers a reduction in emissions by 2035 (around −32.7 Mg/year). According to the Minamata agreement, NP assumes a mercury use reduction in products of 70%. The last scenario is the Maximum Feasible Reduction (MFR). This scenario assumes a significant reduction in anthropogenic emissions (around −59.9 Mg/year). This is because countries could implement all the relevant reduction policies, achieving the most significant possible reduction in each emissions sector [15,62,64]. Within the projected results, by 2035 for the CP scenario, the mercury deposition could decrease by 20 to 30% in Europe and North America. For SH, the deposition would decrease between 5 to 15%. However, in Asia, there would be an increase of up to 50% [62]. In addition, the authors suggested a diminishing of mercury deposition at the global level, including in the SH, by around 20% to 30% for the NP scenario. Despite this, Asia's southern part would increase by between 10% and 15%. However, in the best MFR scenario, the SH would reduce emissions by up to 35% [62].

In contrast, Angot et al. (2018) found more significant mercury reductions in the SH areas. Under similar study conditions, considering that the reduction policies from the year 2020 with the NP scenario would be implemented, they estimated a reduction of 38.3%. In their study, this more significant reduction of mercury emissions occurred because Angot et al. considered a spatial variation of inherited emissions, assuming they were not constant [15].

2.4. Interhemispheric Transport

The NH's most significant anthropogenic emissions are due to the higher industrial development compared to the SH [14,46,59,71]. The most abundant form of atmospheric mercury is GEM, which has low reactivity and solubility. Atmospheric transport is the most significant way this metal is distributed in the environment. Therefore, distribution over long distances depends on its lifetime in the GEM's atmosphere, which is estimated at between 0.5 to 1 year [46]. From this, the interhemispheric transport between the NH and SH may be a relevant aspect when studying atmospheric mercury behaviour, especially in the SH. However, studies have shown that on average, the lifespan of the GEM is around nine months. Therefore, it is shorter than the time determined for an interhemispheric exchange to exist, which is 12 months [77]. Corbitt et al. (2011) presented modelling using GEOS-Chem and a source–receptor influence equation ($I_{ij} = D_{ij}/E_i$), which related the net deposition flux (D) to region j of the emissions of region i, to that of anthropogenic emissions(E) of region i. With this source–receptor influence function, they evaluated the causation of emissions from one region regarding the deposition in another region; therefore, determining the influence of interhemispheric transport on deposition [77]. This study showed a low effect of anthropogenic emissions generated in the NH towards the SH, only influencing the middle tropical zone. In addition, they showed that SH emissions only had a significant influence in this hemisphere, so would not affect the NH to a great extent [77]. Howard et al. (2017) studied interhemispheric transport using the same CTM and two-year GEM measurements from the Australian Tropical Atmospheric Research Station (ATARS). In this study, they determined that the influence of the NH emissions was low and relatively constant, especially in the driest season (April-December). However, 13 days were affected by the transport of emissions from the NH, relating them to a particular increase in the GEM [46]. Despite this, and considering the location of the studied station, that is, the northern part of the SH, there was no significant influence of the emissions from the NH on the SH. This is mainly because this station is at latitudes in the Intertropical Convergence Zone (ITCZ) for which the GEM emissions measured are related more to the emissions from the SH than to those of the NH [46].

Interhemispheric transport of mercury emissions does not significantly affect atmospheric mercury reservoirs. Studies have suggested that it is possible to examine both hemispheres independently [77,78]. Indeed, two factors limit the atmospheric transport of mercury through the equatorial zone. The first is the Hadley circulation, which helps reduce the exchange of air masses at the tropospheric level. The second is because of the existence of the ITCZ [46,78]. The ITCZ is formed in a region where the trade winds of both hemispheres meet and generate a low-pressure zone. This phenomenon generates heavy rains in this zone and rapid vertical movements of air masses, acting as a meteorological barrier for interhemispheric mercury transport. However, in Australia, there are some differences from the other parts of the SH. The upper part of the country is within the limits of the ITCZ, which is associated with the fact that it is in the northern atmospheric hemisphere [46,78].

2.5. Mercury Deposition in the Southern Hemisphere

One of the key processes of the mercury cycle is its atmospheric deposition, which can be of the wet or dry type. Wet deposition comes from precipitation such as rain or snow. Likewise, wet deposition could result from contributions by clouds, dew, and fog [17]. In contrast, dry deposition refers to the mechanism where particles fall to the earth's surface without the intervention of precipitation or some other contributor to wet deposition. With mercury, dry deposition occurs on vegetation, treetops, etc. However, the most important sinks for dry deposition are forest canopies and leaf litter [8,17]. Several authors have studied this type of mercury deposition [17,54,55,59,67,71,79–81]. Despite this, there are still several gaps regarding the measurement methods. Likewise, there is no certainty of the results of the CTM, especially in the SH, because of the few existing data to compare [17]. According to Zhou et al. (2021), global mercury deposition could

be separated into 26–38% for wet deposition and 62–74% for dry deposition. In addition, they identified that vegetation greatly contributes to dry deposition, representing about 76% of the total [18]. Another source is the ocean, one of the main natural mercury sources. The gaseous exchanges between the atmosphere and the ocean generate re-emissions of mercury. Indeed, researchers have argued that these ocean re-emissions have a significant GEM contribution since the ocean covers a great part of the SH. It is estimated that these re-emissions contribute more than half of the atmospheric surface concentration [71].

The mechanism by which mercury can incorporate into biota is principally its deposition as methylmercury. For top predators, it is the main source of mercury due to biomagnification along the food chain [82]. Despite the relevance of measuring and controlling mercury deposition, uncertainty exists in the estimation methods. However, some changes can reduce the uncertainty such as the use of dynamic flux chambers to obtain GEM measurements [17]. This alternative could be used to measure dry deposition in a global network. Also, to improve GOM dry deposition flow modelling it is necessary to enhance the quantification methods of its diverse species [17]. One option for reducing uncertainty in wet deposition flux in CTMs, which is impacted by meteorology, is to conduct an ensemble model study using several meteorological datasets or emissions scenarios [55]. Applying multi-model research with different mercury models using distinct parameterizations is another option for determining the uncertainty in the atmospheric mercury deposition source–receptor relationship [55].

2.5.1. Mercury Wet Deposition

The wet deposition flux ranges between 0.2 and 10 $\mu g/m^2$ per year (annual average of 2.9 $\mu g/m^2$) for the NH and between 1 and 5 $\mu g/m^2$ (annual average of 1.9 $\mu g/m^2$) for the SH. These values vary with diverse factors such as atmospheric mercury concentration, geographic location, weather, precipitation, and atmospheric chemistry [16,55]. In their review, Obrist et al. (2018) stated that there was a significant temporal and spatial variability in Hg's wet deposition (II). Further, they commented that wet deposition followed a similar pattern to the anthropogenic mercury emissions, which would explain these flux differences between the NH and SH [16]. With information from the Global Mercury Observation System (GMOS), Sprovieri et al. (2017) studied five years (2011–2015) of mercury wet deposition data. Their research analysed 17 monitoring stations in the northern and southern hemispheres and was considered the first study of wet deposition that considered the SH. Within the four measurement sites in the SH (AMS, CPT, Cape Grim (CGR), and BAR), the wet deposition flux was lower in comparison with the NH latitudes. However, the flux at CGR was 5 to 10 times higher than at the other SH sites [55,70]. For the NH, they determined a clear relationship between wet deposition and the amount of precipitation. For example, in the year 2014, ISK (Iskrba, Slovenia), with 1631 mm of precipitation, had a wet deposition flux of 10 $\mu g/m^2$ per year, unlike MCH (Mt. Changbai, China) with 177.0 mm, which had an annual deposition of 1.0 $\mu g/m^2$ [55].

In contrast, for the same year in the SH, this relationship was not clear. For example, AMS with 864.1 mm had a deposition of 1.55 $\mu g/m^2$ per year and CGR with 562.3 mm had a deposition of 3.8 $\mu g/m^2$ per year. Therefore, for the SH and low latitudes of the NH (tropical zones), there was no clear relationship between wet deposition and the amount of precipitation compared to the medium and high latitudes of the NH [71]. Regarding wet deposition flux seasonality, there was no apparent relationship between the seasonal variation in rainfall with the total values of the mercury wet deposition flux. Despite this, the authors identified a certain seasonal variability in the SH for the mercury wet deposition flux. This is because most stations obtained low values during the colder seasons and higher values in spring. However, it was not a clear pattern since in BAR, they observed the lowest values in summer [71].

Researchers found some agreements when comparing the measurement results with the models using the CTM. In their presented modelling, Horowitz et al. (2017) verified the existence of the seasonal variability of the wet deposition flux in the NH driven by

the amount of precipitation. Likewise, they showed that including NO_2 and HO_2 as second-stage oxidants improved Hg (II) predictions at lower latitudes, although it still underestimated the magnitude [59]. The results determined that 80% of the global deposition of Hg (II) was in the oceans and 60% of this was wet deposition. Meanwhile, 49% of the total global deposition of Hg (II) was in the tropical oceans, which corresponded to mid-latitudes between $30°$ and $-30°$. In fact, Horowitz et al. (2017) concluded that wet, dry, and total deposition fluxes had higher values in the SH compared to the results by Sprovieri et al. (2017), reaching values close to 15 μg m^{-2} year^{-1} [59,71]. In this sense, Travnikov et al. (2017), using GEOS-Chem, found high deposition values at high latitudes in the SH. They associated these with the intensive oxidation of atmospheric elemental mercury because of the high concentrations of Br. Despite this, they identified Antarctica's lowest mercury wet deposition flux values [14].

Yanxu Zhang et al. (2019) proposed a simulation model coupled with GEOS-Chem to improve wet deposition estimations. This coupled model, MITgcm, uses the chemistry and transport of mercury in the ocean [49]. In their research, they studied the Southern Ocean between 2014 and 2015. They found that the experimental measurements had low zonal variability in elemental mercury concentrations in seawater (ocean) and the atmosphere with values of 0.12 ± 0.067 ng/m^3 and 0.94 ± 0.12 ng/m^3, respectively. In brief, the models implemented in this research largely agreed with the observed values because they had no significant differences [49]. However, when studying the deposition in the SH, the results were higher than those observed. This problem occurred earlier in the simulation performed by Horowitz et al. (2017), reaching values close to 20 μg/m^2 per year in the southern part of Africa and Australia [49,59]. Another problem detected was the discrepancy between the values of elemental mercury concentrations in seawater at the height of the western tropical Pacific Ocean. The maximum values were 50% smaller than the observed data. The main reason for this was that the addition of the cloud mass flux (CMF) was not precise enough. Therefore, the authors suggested using models that could better represent the convective mass flow than the WRF [49].

Although there is concordance between the model estimations and the measurement data regarding the order of magnitude, the models overestimated the wet deposition of mercury in the SH values. Likewise, in the observed data studies, there is some representativeness in the distribution of the measurement sites but there is no specific analysis of other sites that are further away in the SH, such as Antarctica, the middle part of Africa, or the central part of South America. Indeed, in the south-central part of South America, Koening et al. (2021) identified atmospheric mercury levels over the hemispheric average [66]. In a similar vein, Travnikov et al. (2017) revealed an overestimation of the values in the CPT and AMS stations [14]. Finally, Sprovieri et al. (2017), in their research, showed that the data used for the SH was less complete than the HN mercury measurement sites. For instance, few samples were recorded in autumn and summer at the BAR station. This generated more significant uncertainty when comparing the observed and modelled data, which illustrates the importance of further studies on atmospheric mercury in the SH. Despite this, this analysis agrees with that reported by Travnikov et al. (2017). This is because their study concluded that the lowest flows of wet deposition occur in the driest regions, such as Antarctica. Despite this, there is no certainty of the values of dry deposition in the SH for which it is complex to validate the estimates of the models presented [14].

2.5.2. Mercury Dry Deposition

Considering the three forms of mercury in the atmosphere (GEM, GOM, and PBM), it is crucial to clarify the following. For GOM and PBM, both can be subject to wet deposition. However, for dry deposition, these three mercury forms can undertake this process [83]. First, measuring the dry deposition of mercury directly is complex, but some techniques exist to achieve some approximations. Within the measurement techniques, there are substitute surface or leaf litter measurements. Otherwise, CTM to estimate the dry deposition of mercury performs the calculation through the interferential method. This

method is the product of the dry deposition rate and the concentration of atmospheric Hg [8,83]. The CTM has been used mainly to estimate dry deposition in the NH (North America, Asia, and Europe) [8,17,65,69]. Therefore, although the information available on the SH is still scarce, it is related to measurements made or specific mathematical models, especially in Australia.

In the SH, the atmospheric model's results regarding dry mercury deposition have high uncertainty. For instance, some simulations reached values that were between 100 and 400% different to the observed values of dry deposition for GEM [17]. In Australia, the estimation of the dry deposition flux suggests that it is more significant than wet deposition for mercury, with a mean value of $10 \pm 5 \, \mu g/m^2$ per year [70]. However, the mean values were smaller in the simulation at the continental level for the dry deposition flux. The model approximated the dry deposition flux at between 0.5 and 5 $\mu g/m^2$ per year. This value has differences of up to 97% between the maximum and minimum values in each case [70]. Some measurements in Southwest Australia (2017–2018), and Oakdale, New South Wales, have reported seasonal variations in the net deposition flux. This research determined the prevalence of dry deposition during the austral winter. The dry deposition flux reached a maximum value of 0.95 ng/m^2 in one hour in the winter of 2018 [84]. However, this research only presents an analysis of low vegetation (grassland under 2 cm) for which it does not explore other relevant aspects, such as the forest canopy, which is a significant sink for mercury dry deposition [84]. Another area of the SH where there have been deposition studies conducted is South America. In the BAR station in a study carried out by Diéguez et al., the measurements detected GEM levels higher in the austral spring at $0.95 \pm 0.13 \, ng/m^3$ and lower in autumn at $0.8 \pm 0.15 \, ng/m^3$. The average was $0.96 \pm 0.16 \, ng/m^3$, coinciding with the trends presented by Horowitz et al. (2017), where atmospheric mercury levels were higher in the spring [6,59]. Regarding the dry deposition, in that research, the authors showed that the dry deposition of mercury increased during the night, associated with higher humidity values. It correlated with the low levels of GOM. However, it could also be associated with wet deposition, an aspect not mentioned in the study, which is why it was not such an obvious pattern [6].

Another study in Antarctica evaluated the distribution of PBM, seeking to explore the influence of meteorological parameters, seasonal variations, and the flux of dry deposition [85]. In this investigation, it was determined that for the austral summer (2017–2018), the average concentration of PBM in PM_{10} was $51 \pm 27 \, pg/m^3$. Likewise, they found a considerable seasonal variability for the PBM since in November the concentrations were $87 \pm 8 \, pg/m^3$, decreasing around 40% during December and January. When comparing these values with urban areas such as Germany or Spain, the concentration of PBM in Antarctica is at least 20% higher, a significant aspect considering that Antarctica acts as a sink for emissions from the SH [85]. Regarding the dry deposition flux, the authors showed that particles between 2.5 and 10.0 μm generate over 60% of the total dry deposition of PBM. Thus, they suggested that a significant interdependence exists between the dry deposition rate and particle size. They estimated the average PBM flux for the austral summer at 85 ng/m^2 per day for particles between 2.5 and 10.0 μm [85]. There were no other values in the literature on the average flux of PBM, so it was not easy to compare these results. However, considering the previous value as an annual proportion and the summer deposition being a high proportion of the annual flux in coastal areas, we estimated the average PBM flux to be close to 3.1 $\mu g/m^2$ per year. Both values would agree when comparing this flux with another study on the Antarctic with a total average deposition flux of 3.5 $\mu g/m^2$ per year [72]. However, it is difficult to conclude whether the approximation is accurate and conclusive because part of the PBM underwent wet deposition processes, an aspect not measured by Illuminati et al. [74,85].

3. Conclusions and Recommendations

Mercury is a harmful element which garners significant attention because of the diverse health issues it can generate. The Minamata Convention on Mercury is the most relevant

initiative on this matter. To achieve the objectives of the convention, the chemical transport models play a crucial role because they allow studying atmospheric mercury on a diverse scale. In this sense, several researchers have investigated atmospheric mercury by exploring key aspects such as the spatial distribution of mercury, mercury emissions projections, interhemispheric transport, and mercury deposition in the southern hemisphere.

Regarding the spatial distribution of mercury, it is possible to see a particular discrepancy between the observed (measured) and simulated values in the SH. In addition, uncertainty exists regarding the seasonality of gaseous elemental mercury (GEM) and total gaseous mercury (TGM). This issue is due to three key reasons. The first is the scarcity of mercury measurement stations in the SH; in addition to this, they are located far away from each other, so it is complex to analyze the seasonal variations. Another reason is the low amount of research that exists regarding the modelling of mercury in the SH. Atmospheric mercury studies have had a global approach or have been focused on the NH. Therefore, there is a lack of research about the SH in this area. The final reason is the scarcity of data on mercury inventories in the SH. Seasonality does not exist. Therefore, it is more difficult to predict possible seasonal variations in the behaviour of atmospheric mercury using chemical transport models.

Regarding mercury emissions projections, this study reviewed two proposal models. The first, based on the scenarios suggested by the IPCC, showed that there will be an increase in TGM concentrations globally. In addition, it estimated significant changes in the central parts of both hemispheres. In contrast, the estimates made based on reductions according to the Minamata Convention proposals decreased mercury emissions. However, future projections of anthropogenic mercury emissions depend directly on the economic development of each country, especially on the items that are more relevant regarding the emissions of this metal such as the use of fuels for energy. In addition, the low amount of research related to projections of future mercury emissions generates uncertainty regarding the possible global scenarios that could occur. Few papers have been published on the SH regarding mercury emissions projections, especially regarding South America and Africa. This further hinders an accurate understanding of the mercury cycle in this hemisphere. Therefore, this increases uncertainty regarding the real measures that must be implemented to reduce the global balance of mercury.

The transport of interhemispheric anthropogenic emissions of mercury from the NH to the SH does not have a significant impact. The main reason is the existence of the ITCZ, which acts as a meteorological barrier to this transport.

Regarding the deposition, researchers identified high values in the SH and studies suggested the dry deposition is significant. Therefore, this phenomenon is crucial for mercury cycling in the SH, where South America plays a critical role because of the large amount of vegetation. The ocean is another relevant aspect since it is one of the primary sources of natural mercury emissions in the SH because of gaseous exchanges between the atmosphere and the ocean, generating a re-emission of this pollutant.

Wet deposition flux values are lower in the SH than in NH, influenced by anthropogenic emissions. Although in the NH, there is a relationship between wet deposition and the amount of precipitation; the more rain, the greater the wet deposition; however, this relationship in the SH is unclear. Regarding the seasonality of wet deposition, some investigations identified the highest values in the SH during wetter seasons. However, these changes were at different points so a more significant analysis of the behaviour of different areas in the hemisphere is lacking. Finally, the observed data had some agreement with the studied models. Despite this, the maximum values disagreed with this since the wet deposition values estimated using the CTM were much higher than the observed data.

Dry deposition was one of the weakest aspects of the reviewed research on the SH. Comparing the observed data with the results of the CTM studies, there were differences of between 100% and 400%. Thus, research on the dry deposition of mercury in the SH is scarce, for which the results are inconclusive, generating uncertainty regarding the real values.

Although there have been investigations using CTM that have studied the southern hemisphere, there are no studies that focus on this hemisphere. This is because most of the research has focused on the planet's northern hemisphere. In fact, within the studies and reviews, differences were found in both hemispheres regarding both the emissions sources and the sinks. Therefore, it is urgent to enhance the knowledge about the mercury cycle in the SH, since otherwise, there will be low certainty about the variability of the mercury concentration in the atmosphere. This lack of knowledge causes uncertainty regarding the projection of its effects on the population's health and the environment. Finally, among the initiatives promoted by the Minamata Convention is the atmospheric modelling of mercury, a tool that could help improve the knowledge of the mercury cycle in the SH. Therefore, it is crucial to promote research that can study atmospheric mercury and the differences between hemispheres and cover the current research gaps.

Author Contributions: Writing—original draft preparation, J.L.G.; writing—review and editing, J.L.G. and V.C.; validation and review, E.P.-C.; supervision, L.A.D.-R. and F.C.-B.; funding acquisition, F.C.-B. All authors have read and agreed to the published version of the manuscript.

Institutional Review Board Statement: Not applicable.

Informed Consent Statement: Not applicable.

Data Availability Statement: Not applicable.

Conflicts of Interest: The authors declare no conflict of interest.

References

1.　Balakrishnan, K.; Dey, S.; Gupta, T.; Dhaliwal, R.S.; Brauer, M.; Cohen, A.J.; Stanaway, J.D.; Beig, G.; Joshi, T.K.; Aggarwal, A.N.; et al. The impact of air pollution on deaths, disease burden, and life expectancy across the states of India: The Global Burden of Disease Study 2017. *Lancet Planet. Health* **2019**, *3*, e26–e39. [CrossRef]
2.　Kim, K.-H.H.; Kabir, E.; Jahan, S.A. A review on the distribution of Hg in the environment and its human health impacts. *J. Hazard. Mater.* **2016**, *306*, 376–385. [CrossRef] [PubMed]
3.　Chen, C.Y.; Driscoll, C.T.; Eagles-Smith, C.A.; Eckley, C.S.; Gay, D.A.; Hsu-Kim, H.; Keane, S.E.; Kirk, J.L.; Mason, R.P.; Obrist, D.; et al. A Critical Time for Mercury Science to Inform Global Policy. *Environ. Sci. Technol.* **2018**, *52*, 9556–9561. [CrossRef] [PubMed]
4.　Toda, E.; Have, C.T.; Pacyna, J.M. The Minamata Convention. *Chem. Int.* **2020**, *42*, 10–18. [CrossRef]
5.　Lyman, S.N.; Cheng, I.; Gratz, L.E.; Weiss-Penzias, P.; Zhang, L. An updated review of atmospheric mercury. *Sci. Total Environ.* **2019**, *707*, 135575. [CrossRef]
6.　Diéguez, M.C.; Bencardino, M.; García, P.E.; D'Amore, F.; Castagna, J.; De Simone, F.; Soto Cárdenas, C.; Ribeiro Guevara, S.; Pirrone, N.; Sprovieri, F. A multi-year record of atmospheric mercury species at a background mountain station in Andean Patagonia (Argentina): Temporal trends and meteorological influence. *Atmos. Environ.* **2019**, *214*, 116819. [CrossRef]
7.　Slemr, F.; Martin, L.; Labuschagne, C.; Mkololo, T.; Angot, H.; Magand, O.; Magand, O.; Garat, P.; Ramonet, M.; Bieser, J. Atmospheric mercury in the Southern Hemisphere—Part 1: Trend and inter-annual variations in atmospheric mercury at Cape Point, South Africa, in 2007–2017, and on Amsterdam Island in 2012–2017. *Atmos. Chem. Phys.* **2020**, *20*, 7683–7692. [CrossRef]
8.　Wright, L.; Zhang, L.; Marsik, F.J. Overview of mercury dry deposition, litterfall, and throughfall studies. *Atmos. Chem. Phys.* **2016**, *16*, 13399–13416. [CrossRef]
9.　Gworek, B.; Dmuchowski, W.; Baczewska, A.H.; Brągoszewska, P.; Bemowska-Kałabun, O.; Wrzosek-Jakubowska, J. Air Contamination by Mercury, Emissions and Transformations—A Review. *Water Air Soil Pollut.* **2017**, *228*, 123. [CrossRef]
10.　Subir, M.; Ariya, P.A.; Dastoor, A.P. A review of uncertainties in atmospheric modeling of mercury chemistry I. Uncertainties in existing kinetic parameters e Fundamental limitations and the importance of heterogeneous chemistry. *Atmos. Environ.* **2011**, *45*, 5664–5676. [CrossRef]
11.　Si, L.; Ariya, P.A. Recent Advances in Atmospheric Chemistry of Mercury. *Atmosphere* **2018**, *9*, 76. [CrossRef]
12.　Zhang, Y.; Bocquet, M.; Mallet, V.; Seigneur, C.; Baklanov, A. Real-time air quality forecasting, part I: History, techniques, and current status. *Atmos. Environ.* **2012**, *60*, 632–655. [CrossRef]

13. Zaid Abualkishik, A. A comparative study on the software architecture of WRF and other numerical weather prediction models. *J. Theor. Appl. Inf. Technol.* **2018**, *31*, 24.

14. Travnikov, O.; Angot, H.; Artaxo, P.; Bencardino, M.; Bieser, J.; D'Amore, F.; Dastoor, A.; De Simone, F.; DIéguez, M.C.; Dommergue, A.; et al. Multi-model study of mercury dispersion in the atmosphere: Atmospheric processes and model evaluation. *Atmos. Chem. Phys.* **2017**, *17*, 5271–5295. [CrossRef]

15. Angot, H.; Hoffman, N.; Giang, A.; Thackray, C.P.; Hendricks, A.N.; Urban, N.R.; Selin, N.E. Global and Local Impacts of Delayed Mercury Mitigation Efforts. *Environ. Sci. Technol.* **2018**, *52*, 12968–12977. [CrossRef] [PubMed]

16. Obrist, D.; Kirk, J.L.; Zhang, L.; Sunderland, E.M.; Jiskra, M.; Selin, N.E. A review of global environmental mercury processes in response to human and natural perturbations: Changes of emissions, climate, and land use. *Ambio* **2018**, *47*, 116–140. [CrossRef] [PubMed]

17. Zhang, L.; Zhou, P.; Cao, S.; Zhao, Y. Atmospheric mercury deposition over the land surfaces and the associated uncertainties in observations and simulations: A critical review. *Atmos. Chem. Phys.* **2019**, *19*, 15587–15608. [CrossRef]

18. Zhou, J.; Obrist, D.; Dastoor, A.; Jiskra, M.; Ryjkov, A. Vegetation uptake of mercury and impacts on global cycling. *Nat. Rev. Earth Environ.* **2021**, *2*, 269–284. [CrossRef]

19. Falakdin, P.; Terzaghi, E.; Di Guardo, A. Spatially resolved environmental fate models: A review. *Chemosphere* **2022**, *290*, 133394. [CrossRef]

20. Zhang, P.; Zhang, Y. Earth system modeling of mercury using CESM2—Part 1: Atmospheric model CAM6-Chem/Hg v1.0. *Geosci. Model Dev.* **2022**, *15*, 3587–3601. [CrossRef]

21. AMAP; UN Environment. *Technical Background Report for the Global Mercury Assessment 2018*; Arctic Monitoring and Assessment Programme: Oslo, Norway; UN Environment Programme, Chemicals and Health Branch: Geneva, Switzerland, 2019; pp. viii + 426.

22. Kos, G.; Ryzhkov, A.; Dastoor, A.; Narayan, J.; Steffen, A.; Ariya, P.A.; Zhang, L. Evaluation of discrepancy between measured and modelled oxidized mercury species mercury species. *Atmos. Chem. Phys* **2013**, *13*, 4839–4863. [CrossRef]

23. De Simone, F.; D'Amore, F.; Bencardino, M.; Carbone, F.; Hedgecock, I.M.; Sprovieri, F.; Cinnirella, S.; Pirrone, N. The GOS4M Knowledge Hub: A web-based effectiveness evaluation platform in support of the Minamata Convention on Mercury. *Environ. Sci. Policy* **2021**, *124*, 235–246. [CrossRef]

24. Charv At, P.; Klime, L.; Pospíšil, J.; Kleme, J.; Varbanov, S. An overview of mercury emissions in the energy industry-A step to mercury footprint assessment. *J. Clean. Prod.* **2020**, *267*, 122087. [CrossRef]

25. Steenhuisen, F.; Wilson, S.J. Development and application of an updated geospatial distribution model for gridding 2015 global mercury emissions. *Atmos. Environ.* **2019**, *211*, 138–150. [CrossRef]

26. De Simone, F.; Hedgecock, I.M.; Carbone, F.; Cinnirella, S.; Sprovieri, F.; Pirrone, N. Estimating Uncertainty in Global Mercury Emission Source and Deposition Receptor Relationships. *Atmosphere* **2017**, *8*, 236. [CrossRef]

27. AMAP; UN Environment. *Technical Background Report for the Global Mercury Assessment*; United Nations Environment Programme: Nairobi, Kenya, 2013.

28. Pirrone, N.; Cinnirella, S.; Feng, X.; Finkelman, R.B.; Friedli, H.R.; Leaner, J.; Mason, R.; Mukherjee, A.B.; Stracher, G.B.; Streets, D.G.; et al. Global mercury emissions to the atmosphere from anthropogenic and natural sources. *Atmos. Chem. Phys.* **2010**, *10*, 5951–5964. [CrossRef]

29. Sundseth, K.; Pacyna, J.M.; Pacyna, E.G.; Pirrone, N.; Thorne, R.J. Global Sources and Pathways of Mercury in the Context of Human Health. *Int. J. Environ. Res. Public Health* **2017**, *14*, 105. [CrossRef]

30. Shi, Y.; Zhao, A.; Matsunaga, T.; Yamaguchi, Y.; Zang, S.; Li, Z.; Yu, T.; Gu, X. High-resolution inventory of mercury emissions from biomass burning in tropical continents during 2001–2017. *Sci. Total Environ.* **2019**, *653*, 638–648. [CrossRef] [PubMed]

31. Friedli, H.R.; Arellano, A.F.; Cinnirella, S.; Pirrone, N. Mercury emissions from global biomass burning: Spatial and temporal distribution. In *Mercury Fate and Transport in the Global Atmosphere*; Springer: Boston, MA, USA, 2009; pp. 193–220. [CrossRef]

32. Driscoll, C.T.; Mason, R.P.; Chan, H.M.; Jacob, D.J.; Pirrone, N. Mercury as a Global Pollutant: Sources, Pathways, and Effects. *Environ. Sci. Technol.* **2013**, *47*, 4967–4983. [CrossRef]

33. Zhang, Y.; Song, Z.; Huang, S.; Zhang, P.; Peng, Y.; Wu, P.; Gu, J.; Dutkiewicz, S.; Zhang, H.; Wu, S.; et al. Global health effects of future atmospheric mercury emissions. *Nat. Commun.* **2021**, *12*, 3035. [CrossRef]

34. Peplow, D.; Augustine, S. Neurological abnormalities in a mercury exposed population among indigenous Wayana in Southeast Suriname. *Environ. Sci. Process. Impacts* **2014**, *16*, 2415–2422. [CrossRef] [PubMed]

35. Clarkson, T.W.; Magos, L.; Myers, G.J. The toxicology of mercury—Current exposures and clinical manifestations. *N. Engl. J. Med.* **2003**, *349*, 1731–1737. [CrossRef] [PubMed]

36. Bernhoft, R.A. Mercury toxicity and treatment: A review of the literature. *J. Environ. Public Health* **2012**, *2012*, 460508. [CrossRef] [PubMed]

37. Guallar, E.; Sanz-Gallardo, M.I.; Veer, P.V.T.; Bode, P.; Aro, A.; Gómez-Aracena, J.; Kark, J.D.; Riemersma, R.A.; Martín-Moreno, J.M.; Kok, F.J. Mercury, Fish Oils, and the Risk of Myocardial Infarction. *N. Engl. J. Med.* **2009**, *347*, 1747–1754. [CrossRef] [PubMed]

38. Nakazawa, K.; Nagafuchi, O.; Kawakami, T.; Inoue, T.; Elvince, R.; Kanefuji, K.; Nur, I.; Napitupulu, M.; Basir-Cyio, M.; Kinoshita, H.; et al. Human health risk assessment of atmospheric mercury inhalation around three artisanal small-scale gold mining areas in Indonesia. *Environ. Sci. Atmos.* **2021**, *1*, 423–433. [CrossRef]

39. Pavilonis, B.; Grassman, J.; Johnson, G.; Diaz, Y.; Caravanos, J. Characterization and risk of exposure to elements from artisanal gold mining operations in the Bolivian Andes. *Environ. Res.* **2017**, *154*, 1–9. [CrossRef]

40. Bose-O'reilly, S.; Drasch, G.; Beinhoff, C.; Tesha, A.; Drasch, K.; Roider, G.; Taylor, H.; Appleton, D.; Siebert, U. Health assessment of artisanal gold miners in Tanzania. *Sci. Total Environ.* **2009**, *408*, 796–805. [CrossRef]

41. Ohlander, J.; Huber, S.M.; Schomaker, M.; Heumann, C.; Schierl, R.; Michalke, B.; Jenni, O.G.; Caflisch, J.; Muñoz, D.M.; von Ehrenstein, O.S.; et al. Mercury and neuromotor function among children in a rural town in Chile. *Int. J. Occup. Environ. Health* **2016**, *22*, 27–35. [CrossRef]

42. Leiva González, J.; Onederra, I. Environmental Management Strategies in the Copper Mining Industry in Chile to Address Water and Energy Challenges-Review. *Mining* **2022**, *2*, 197–232. [CrossRef]

43. Hrubá, F.; Strömberg, U.; Černá, M.; Chen, C.; Harari, F.; Harari, R.; Horvat, M.; Koppová, K.; Kos, A.; Krsková, A.; et al. Blood cadmium, mercury, and lead in children: An international comparison of cities in six European countries, and China, Ecuador, and Morocco. *Environ. Int.* **2012**, *41*, 29–34. [CrossRef]

44. Laborde, A.; Tomasina, F.; Bianchi, F.; Bruné, M.N.; Buka, I.; Comba, P.; Corra, L.; Cori, L.; Duffert, C.M.; Harari, R.; et al. Children's health in Latin America: The infuence of environmental exposures. *Environ. Health Perspect.* **2015**, *123*, 201–209. [CrossRef]

45. González-Carrasco, V.; Velasquez-Lopez, P.C.; Olivero-Verbel, J.; Pájaro-Castro, N. Air Mercury Contamination in the Gold Mining Town of Portovelo, Ecuador. *Bull. Environ. Contam. Toxicol.* **2011**, *87*, 250–253. [CrossRef] [PubMed]

46. Zhang, Y.; Jaeglé, L.; Thompson, L.A.; Streets, D.G. Six centuries of changing oceanic mercury. *Glob. Biogeochem. Cycles* **2014**, *28*, 1251–1261. [CrossRef]

47. Muntean, M.; Janssens-Maenhout, G.; Song, S.; Giang, A.; Selin, N.E.; Zhong, H.; Zhao, Y.; Olivier, J.G.J.; Guizzardi, D.; Crippa, M.; et al. Evaluating EDGARv4.tox2 speciated mercury emissions ex-post scenarios and their impacts on modelled global and regional wet deposition patterns. *Atmos. Environ.* **2018**, *184*, 56–68. [CrossRef]

48. Shah, V.; Jacob, D.J.; Thackray, C.P.; Wang, X.; Sunderland, E.M.; Dibble, T.S.; Saiz-Lopez, A.; Černušák, I.; Kellö, V.; Castro, P.J.; et al. Improved Mechanistic Model of the Atmospheric Redox Chemistry of Mercury. *Environ. Sci. Technol.* **2021**, *55*, 13. [CrossRef] [PubMed]

49. Zhang, H.; Wu, S.; Leibensperger, E.M. Source-receptor relationships for atmospheric mercury deposition in the context of global change. *Atmos. Environ.* **2021**, *254*, 118349. [CrossRef]

50. Zhang, H.; Holmes, C.D.; Wu, S. Impacts of changes in climate, land use and land cover on atmospheric mercury. *Atmos. Environ.* **2016**, *141*, 230–244. [CrossRef]

51. Kumar, A.; Wu, S. Mercury Pollution in the Arctic from Wildfires: Source Attribution for the 2000s. *Environ. Sci. Technol.* **2019**, *53*, 11269–11275. [CrossRef] [PubMed]

52. Huang, S.; Zhang, Y. Interannual Variability of Air-Sea Exchange of Mercury in the Global Ocean: The "seesaw Effect" in the Equatorial Pacific and Contributions to the Atmosphere. *Environ. Sci. Technol.* **2021**, *55*, 7145–7156. [CrossRef]

53. Horowitz, H.; Jacob, D.; Zhang, Y.; DIbble, T.S.; Slemr, F.; Amos, H.M.; Schmidt, J.A.; Corbitt, E.S.; Marais, E.A.; Sunderland, E.M. A new mechanism for atmospheric mercury redox chemistry: Implications for the global mercury budget. *Atmos. Chem. Phys.* **2017**, *17*, 6353–6371. [CrossRef]

54. Howard, D.; Nelson, P.F.; Edwards, G.C.; Morrison, A.L.; Fisher, J.A.; Ward, J.; Harnwell, J.; Van Der Schoot, M.; Atkinson, B.; Chambers, S.D.; et al. Atmospheric mercury in the Southern Hemisphere tropics: Seasonal and diurnal variations and influence of inter-hemispheric transport. *Atmos. Chem. Phys.* **2017**, *17*, 11623–11636. [CrossRef]

55. Holmes, C.D.; Jacob, D.J.; Corbitt, E.S.; Mao, J.; Yang, X.; Talbot, R.; Slemr, F. Global atmospheric model for mercury including oxidation by bromine atoms. *Atmos. Chem. Phys.* **2010**, *10*, 12037–12057. [CrossRef]

56. Dibble, T.S.; Tetu, H.L.; Jiao, Y.; Thackray, C.P.; Jacob, D.J. Modeling the OH-Initiated Oxidation of Mercury in the Global Atmosphere without Violating Physical Laws. *J. Phys. Chem. A* **2020**, *124*, 444–453. [CrossRef] [PubMed]

57. Zhang, Y.; Horowitz, H.; Wang, J.; Xie, Z.; Kuss, J.; Soerensen, A.L. A Coupled Global Atmosphere-Ocean Model for Air-Sea Exchange of Mercury: Insights into Wet Deposition and Atmospheric Redox Chemistry. *Environ. Sci. Technol.* **2019**, *53*, 5052–5061. [CrossRef] [PubMed]

58. Shah, V.; Jaeglé, L. Subtropical subsidence and surface deposition of oxidized mercury produced in the free troposphere. *Atmos. Chem. Phys.* **2017**, *17*, 8999–9017. [CrossRef]

59. Strode, S.A.; Jaeglé, L.; Selin, N.E.; Jacob, D.J.; Park, R.J.; Yantosca, R.M.; Mason, R.P.; Slemr, F. Air-sea exchange in the global mercury cycle. *Glob. Biogeochem. Cycles* **2007**, *21*, 1017. [CrossRef]

60. Schofield, R.; Utembe, S.; Gionfriddo, C.; Tate, M.; Krabbenhoft, D.; Adeloju, S.; Keywood, M.; Dargaville, R.; Sandiford, M. Atmospheric mercury in the Latrobe Valley, Australia: Case study June 2013. *Elementa* **2021**, *9*, 00072. [CrossRef]

61. Bieser, J.; Slemr, F.; Ambrose, J.; Brenninkmeijer, C.; Brooks, S.; Dastoor, A.; Desimone, F.; Ebinghaus, R.; Gencarelli, C.N.; Geyer, B.; et al. Multi-model study of mercury dispersion in the atmosphere: Vertical and interhemispheric distribution of mercury species. *Atmos. Chem. Phys.* **2017**, *17*, 6925–6955. [CrossRef]

62. Pacyna, J.M.; Travnikov, O.; De Simone, F.; Hedgecock, I.M.; Sundseth, K.; Pacyna, E.G.; Steenhuisen, F.; Pirrone, N.; Munthe, J.; Kindbom, K. Current and future levels of mercury atmospheric pollution on a global scale. *Atmos. Chem. Phys.* **2016**, *16*, 12495–12511. [CrossRef]

63. De Simone, F.; Gencarelli, C.N.; Hedgecock, I.M.; Pirrone, N. A Modeling Comparison of Mercury Deposition from Current Anthropogenic Mercury Emission Inventories. *Environ. Sci. Technol.* **2016**, *50*, 5154–5162. [CrossRef] [PubMed]
64. De Simone, F.; Artaxo, P.; Bencardino, M.; Cinnirella, S.; Carbone, F.; D'Amore, F.; Dommergue, A.; Bin Feng, X.; Gencarelli, C.N.; Hedgecock, I.M.; et al. Particulate-phase mercury emissions from biomass burning and impact on resulting deposition: A modelling assessment. *Atmos. Chem. Phys.* **2017**, *17*, 1881–1899. [CrossRef]
65. De Simone, F.; Gencarelli, C.N.; Hedgecock, I.M.; Pirrone, N. Global atmospheric cycle of mercury: A model study on the impact of oxidation mechanisms. *Environ. Sci. Pollut. Res.* **2014**, *21*, 4110–4123. [CrossRef] [PubMed]
66. Koenig, A.M.; Magand, O.; Laj, P.; Andrade, M.; Moreno, I.; Velarde, F.; Salvatierra, G.; Gutierrez, R.; Blacutt, L.; Aliaga, D.; et al. Seasonal patterns of atmospheric mercury in tropical South America as inferred by a continuous total gaseous mercury record at Chacaltaya station (5240 m) in Bolivia. *Atmos. Chem. Phys* **2021**, *21*, 3447–3472. [CrossRef]
67. Jiskra, M.; Sonke, J.E.; Obrist, D.; Bieser, J.; Ebinghaus, R.; Myhre, C.L.; Pfaffhuber, K.A.; Wängberg, I.; Kyllönen, K.; Worthy, D.; et al. A vegetation control on seasonal variations in global atmospheric mercury concentrations. *Nat. Geosci.* **2018**, *11*, 244–250. [CrossRef]
68. Sprovieri, F.; Pirrone, N.; Bencardino, M.; D'Amore, F.; Carbone, F.; Cinnirella, S.; Mannarino, V.; Landis, M.; Ebinghaus, R.; Weigelt, A.; et al. Atmospheric mercury concentrations observed at ground-based monitoring sites globally distributed in the framework of the GMOS network. *Atmos. Chem. Phys.* **2016**, *16*, 11915–11935. [CrossRef] [PubMed]
69. Song, S.; Selin, N.E.; Soerensen, A.L.; Angot, H.; Artz, R.; Brooks, S.; Brunke, E.-G.; Conley, G.; Dommergue, A.; Ebinghaus, R.; et al. Top-down constraints on atmospheric mercury emissions and implications for global biogeochemical cycling. *Atmos. Chem. Phys.* **2015**, *15*, 7103–7125. [CrossRef]
70. Fisher, J.A.; Nelson, P.F. Atmospheric mercury in Australia: Recent findings and future research needs. *Elem. Sci. Anthr.* **2020**, *8*, 070. [CrossRef]
71. Sprovieri, F.; Pirrone, N.; Bencardino, M.; D'Amore, F.; Angot, H.; Barbante, C.; Brunke, E.G.; Arcega-Cabrera, F.; Cairns, W.; Comero, S.; et al. Five-year records of mercury wet deposition flux at GMOS sites in the Northern and Southern hemispheres. *Atmos. Chem. Phys.* **2017**, *17*, 2689–2708. [CrossRef]
72. Slemr, F.; Angot, H.; Dommergue, A.; Magand, O.; Barret, M.; Weigelt, A.; Ebinghaus, R.; Brunke, E.G.; Pfaffhuber, K.A.; Edwards, G.; et al. Comparison of mercury concentrations measured at several sites in the Southern Hemisphere. *Atmos. Chem. Phys.* **2015**, *15*, 3125–3133. [CrossRef]
73. Soerensen, A.L.; Skov, H.; Jacob, D.J.; Soerensen, B.T.; Johnson, M.S. Global concentrations of gaseous elemental mercury and reactive gaseous mercury in the marine boundary layer. *Environ. Sci. Technol.* **2010**, *44*, 7425–7430. [CrossRef]
74. Angot, H.; Magand, O.; Helmig, D.; Ricaud, P.; Quennehen, B.; Gallée, H.; Del Guasta, M.; Sprovieri, F.; Pirrone, N.; Savarino, J.; et al. New insights into the atmospheric mercury cycling in central Antarctica and implications on a continental scale. *Atmos. Chem. Phys.* **2016**, *16*, 8249–8264. [CrossRef]
75. Miller, M.B.; Howard, D.A.; Pierce, A.M.; Cook, K.R.; Keywood, M.; Powell, J.; Gustin, M.S.; Edwards, G.C. Atmospheric reactive mercury concentrations in coastal Australia and the Southern Ocean. *Sci. Total Environ.* **2021**, *751*, 141681. [CrossRef] [PubMed]
76. Lei, H.; Wuebbles, D.J.; Liang, X.-Z.; Tao, Z.; Olsen, S.; Artz, R.; Ren, X.; Cohen, M. Atmospheric Chemistry and Physics Projections of atmospheric mercury levels and their effect on air quality in the United States. *Atmos. Chem. Phys* **2014**, *14*, 783–795. [CrossRef]
77. Corbitt, E.S.; Jacob, D.J.; Holmes, C.D.; Streets, D.G.; Sunderland, E.M. Global source-receptor relationships for mercury deposition under present-day and 2050 emissions scenarios. *Environ. Sci. Technol.* **2011**, *45*, 10477–10484. [CrossRef]
78. Hamilton, J.F.; Allen, G.; Watson, N.M.; Lee, J.D.; Saxton, J.E.; Lewis, A.C.; Vaughan, G.; Bower, K.N.; Flynn, M.J.; Crosier, J.; et al. Observations of an atmospheric chemical equator and its implications for the tropical warm pool region. *J. Geophys. Res. Atmos.* **2008**, *113*, D20313. [CrossRef]
79. Li, C.; Sonke, J.E.; Roux, L.; Piotrowska, N.; Van der Putten, N.; Roberts, S.J.; Daley, T.; Rice, E.; Gehrels, R.; Enrico, M.; et al. Unequal Anthropogenic Enrichment of Mercury in Earth's Northern and Southern Hemispheres. *ACS Earth Sp. Chem.* **2020**, *4*, 2073–2081. [CrossRef]
80. Li, F.; Ma, C.; Zhang, P. Mercury Deposition, Climate Change and Anthropogenic Activities: A Review. *Front. Earth Sci.* **2020**, *8*, 316. [CrossRef]
81. Saiz-Lopez, A.; Travnikov, O.; Sonke, J.E.; Thackray, C.P.; Jacob, D.J.; Carmona-García, J.; Francés-Monerris, A.; Roca-Sanjuán, D.; Acuña, A.U.; Dávalos, J.Z.; et al. Photochemistry of oxidized Hg(I) and Hg(II) species suggests missing mercury oxidation in the troposphere. *Proc. Natl. Acad. Sci. USA* **2020**, *117*, 30949–30956. [CrossRef]
82. Cossa, D.; Knoery, J.; Bǎnaru, D.; Harmelin-Vivien, M.; Sonke, J.E.; Hedgecock, I.M.; Bravo, A.G.; Rosati, G.; Canu, D.; Horvat, M.; et al. Mediterranean Mercury Assessment 2022: An Updated Budget, Health Consequences. *Environ. Sci. Technol.* **2022**, *56*, 3840–3862. [CrossRef] [PubMed]
83. Wright, L.P.; Zhang, L.; Cheng, I.; Aherne, J.; Wentworth, G.R. Impacts and Effects Indicators of Atmospheric Deposition of Major Pollutants to Various Ecosystems—A Review. *Aerosol Air Qual. Res.* **2018**, *18*, 1953–1992. [CrossRef]
84. MacSween, K.; Edwards, G.C.; Beggs, P.J. Seasonal gaseous elemental mercury fluxes at a terrestrial background site in south-eastern Australia. *Elem. Sci. Anthr.* **2020**, *8*, 27. [CrossRef]
85. Illuminati, S.; Annibaldi, A.; Bau, S.; Scarchilli, C.; Ciardini, V.; Grigioni, P.; Girolametti, F.; Vagnoni, F.; Scarponi, G.; Truzzi, C. Seasonal Evolution of Size-Segregated Particulate Mercury in the Atmospheric Aerosol Over Terra Nova Bay, Antarctica. *Molecules* **2020**, *25*, 3971. [CrossRef] [PubMed]